applied sciences

MDPI

Article

Estimation of Impact Loads Transmitted to Vibro-Ripper Housing Using Transfer Path Analysis

Daeji Kim [1,2], Hyune-Jun Park [1], Joo-Young Oh [1], Jung-Woo Cho [1], Jintai Chung [2,*] and Changheon Song [1,*]

[1] Advanced Mechatronics R&D Group, Korea Institute of Industrial Technology, Daegu 42994, Republic of Korea; kimdaeji@kitech.re.kr (D.K.); goldneiya@kitech.re.kr (H.-J.P.); jyoh@kitech.re.kr (J.-Y.O.); chojw1665@kitech.re.kr (J.-W.C.)
[2] Department of Mechanical Engineering, Hanyang University, Ansan 15588, Republic of Korea
* Correspondence: jchung@hanyang.ac.kr (J.C.); sch8310@kitech.re.kr (C.S.)

Abstract: This study aimed to estimate impact loads delivered to vibro-ripper housing through link modules, together with loads transmitted in various directions. Housing vibration resulting from impact loads generated during the operating condition and frequency response functions were assessed by vibration and modal experiments, respectively. Vibration data and transfer functions were applied in a transfer path analysis (TPA) model to analyze the quantified impact loads transmitted through the key components of the vibro-ripper to its housing. Impact loads derived by TPA for different housing parts were compared with those in the tooth derived from load-cell measurements, validating the TPA method. As a result of the verification, the impact load calculated by the TPA method was 193.7 kN, whereas that from the striking force measured by the load cell was 220 kN, a difference of 12.3%. The results of this study may be important input values for numerical analysis in equipment design and can be used as key data for structural safety evaluation and optimization. In summary, this paper introduces the vibration-based TPA method and considers its applicability to construction machinery exposed to impact vibration and loads.

Keywords: vibro-ripper; impact load; vibration experiment; transfer path analysis; load estimation

Citation: Kim, D.; Park, H.-J.; Oh, J.-Y.; Cho, J.-W.; Chung, J.; Song, C. Estimation of Impact Loads Transmitted to Vibro-Ripper Housing Using Transfer Path Analysis. *Appl. Sci.* **2023**, *13*, 10990. https://doi.org/10.3390/app131910990

Academic Editor: Marco Troncossi

Received: 8 September 2023
Revised: 26 September 2023
Accepted: 27 September 2023
Published: 5 October 2023

1. Introduction

Vibro-rippers attached to excavators are used for various purposes including rock crushing, ground fracturing, structure demolition, and bedrock to produce material or aggregates at construction and mining sites. The size, structure, and major components of a vibro-ripper are illustrated in Figure 1. A vibro-ripper comprises a coupler mounted on an excavator, the isolation rubber to isolate the vibration transmitted to the excavator arm and boom, the directional control valve to control the direction of hydraulic fluid, a pair of eccentric gears in the gearbox, a hydraulic motor that transmits the driving force of the eccentric gear through hydraulic energy during operation, a link module that transmits the excitation force generated by the eccentric gear to the shank and tooth, and a tooth that breaks the rock directly. In operation, a driving force is transmitted to the drive shaft of the gearbox by a hydraulic motor. The drive shaft of the gearbox comprises of a pair of gears and an eccentric weight. The eccentric rotational motion of the drive shaft crushes the rock through the impact of the shank and tooth attached to the gearbox.

Previous studies have examined vibro-ripper systems. Jonck and Slabbert [1] undertook failure analysis of an induction-hardened spur gear of a vibro-hammer, and Chen et al. [2] studied the development and application of vibratory driving techniques using a high-frequency hydraulic vibratory hammer. Xu et al. [3] simulated the problem of vibration in an impact ripper working under the excitation force of a hydraulic ripper, and Oh et al. [4] investigated the fatigue life of welded joints on the gearbox shank in a vibro-ripper. Lee et al. [5] studied mechanical vibrations in vibro-hammers.

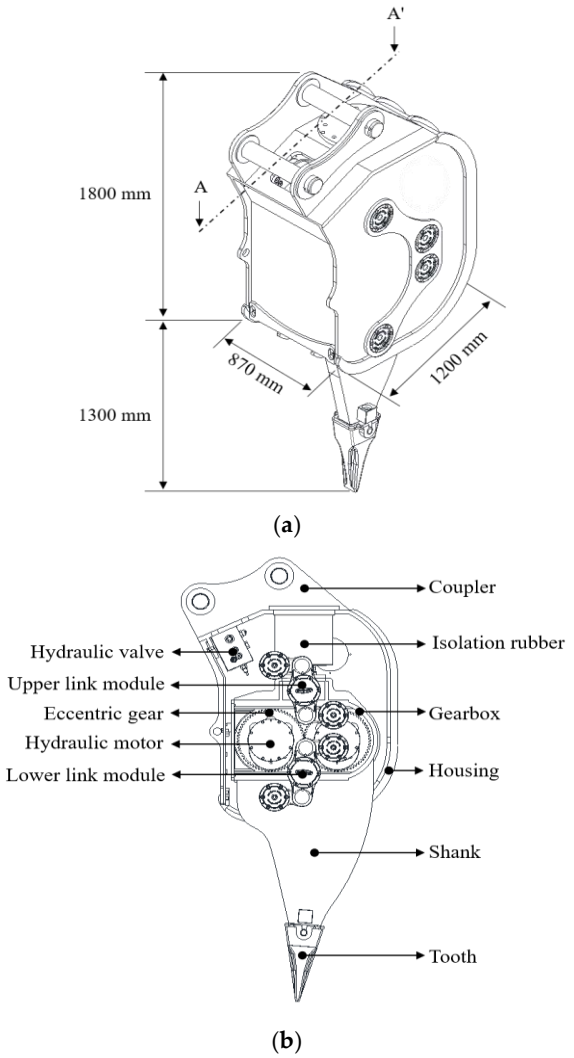

Figure 1. Schematic diagram of a vibro-ripper: (**a**) isometric view, (**b**) cross-section A–A′.

In previous investigations of rock crushing systems, Ficarella et al. [6–8] employed a one-dimensional hydraulic simulation and experiments to assess the performance and design method of a hydraulic breaker, while others have focused on improvements to impact performance, minimizing the weight of the breaker housing, and design optimization [9–11]. Other studies have focused on the development and improvement of vibro-ripper and hammer systems. Impact loads of mechanical devices have also been studied. Song et al. [12] undertook a quantitative assessment of the impact loads transmitted to the housing of a hydraulic breaker. The authors confirmed the feasibility of the TPA method by comparing the quantified impact loads with the impact energy of the chisel. Other studies have examined the measurement of impact loads, including the use of sensors (e.g., load cells and strain gauges) to assess the impact vibration of a structure, and calculations of structural damage resulting from impact or excitation loads [13–19].

Previous studies have focused mainly on fatigue life prediction through failure analysis of major parts of vibration rippers; dynamic response analysis of vibration rippers through driving technology, optimal equipment operation, and vibration analysis; and the durability of welded structures. However, there has been no estimation of impact loads transmitted to parts of a vibro-ripper during the crushing of rocks with eccentric rotational motion.

Of the key factors that regulate the durability and performance of a vibro-ripper, (e.g., welding structural stability, shank and tooth strength, wear, and the hydraulic system), the stability of parts constituting the structure of the ripper is crucial due to its direct

relationship to machine durability. Impact loads incurred during rock crushing directly affect the structural stability of the crusher and the durability of its components [12,20]. Prediction of the structural stability of a vibro-ripper, its durability, and life cycle span requires analysis of the impact load generated during rock crushing and transmitted to the housing through each part of the system. The crushing of rocks through rotational motion exposes the vibro-ripper to an extreme work environment involving continuous impact vibration and load. Therefore, loads transmitted during rock crushing must be quantitatively analyzed to verify the structural stability and design robustness of core parts of the crusher, which are closely related to its durability and performance. The quantitative load is a reference value for the design strength of the major parts of construction equipment and for the input load used in durability evaluation.

This study sought to assess the impact load transmitted through the link modules of the vibro-ripper to the housing and the impact load transmitted in different directions. In this context, this study aimed to analyze and quantify the contributions of impact load to different parts of a vibro-ripper, and the transmission of loads during rock crushing work. To that end, Section 2 of this paper explains the theoretical background of the transfer path analysis method for impact load estimation and vibration experiments of a vibro-ripper. Section 3 presents the quantitative load estimation results using the TPA method and compares them with the striking force measured through the load cell. The research concludes with Section 4.

Impact loads are transmitted to each part of a vibro-ripper through vibrational effects such as pitch, roll, and yaw motion (Figure 2). We applied vibration-based transfer path analysis (TPA) in considering triaxial vibrational characteristics to quantify the striking load during crushing work that is ultimately transmitted to the ripper housing through the link modules. We further analyzed the contribution of the transmitted impact load. The impact loads of each structural part, as derived using the TPA method, were compared with those in the vibro-ripper tooth derived from the operating load of a ripper, measured using a load cell. This comparison confirmed the applicability of the TPA method to mechanical systems subjected to impact loads and vibration.

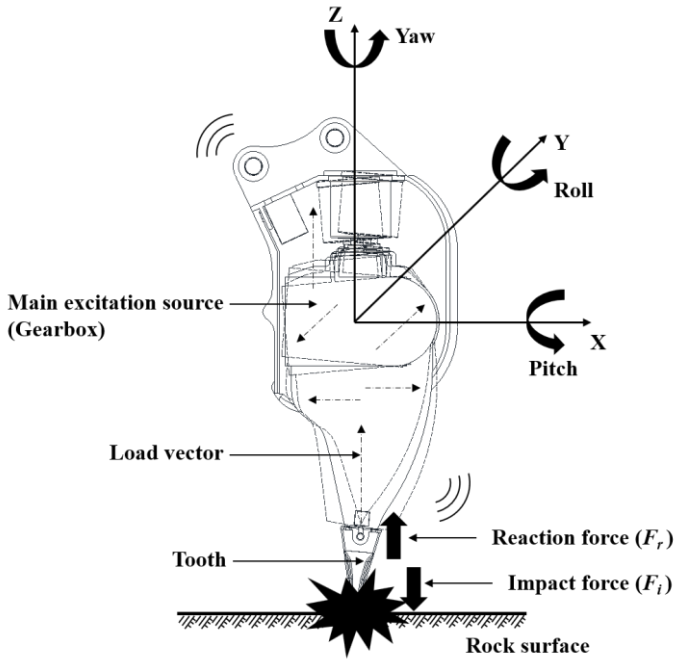

Figure 2. Triaxial vibration of a vibro-ripper during rock crushing.

2. Vibration Experiments with a Vibro-Ripper

2.1. Theoretical Background of Transfer Path Analysis

The TPA method is employed to investigate the main transfer paths of mechanical systems of acoustic and acceleration energy generated by an excitation source. The sensitivity of each component to the transfer path can be quantified through experiments [12,21]. This approach takes account of air- and structure-borne noises [12,22]. The latter is caused by structure vibration, whereas the former is transmitted through the air. A microphone or acoustic receiver is used to measure these noise components. The governing equation of the TPA method for each system component is given in Equation (1). The respective noise and vibration can be defined as the product of the transfer functions about the excitation source and transfer path as [12]:

$$P_t(\omega) = \sum_{i=1}^{n} VTF_i(\omega) \cdot F_i(\omega) + \sum_{j=1}^{r} NTF_j(\omega) \cdot Q_j(\omega) \quad (1)$$

where F_i (i = 1,. . ., n) represents the interfacial forces arising from structural vibration loads, Q_j (j = 1,. . ., r) denotes the volume velocities related to acoustic loads, NTF_j is the transfer function for noise, and VTF_i is the transfer function for structural vibrations. The TPA method is divided into a passive subsystem (the transfer path and receiver positions) and a global subsystem (noise and vibration sources) (Figure 3). At the interface between the two subsystems, acoustic or structural loads can be defined according to the type of coupling. The excitations are propagated to receiver points along the paths. The loads are typically interface forces (F) or volume velocities (Q) (e.g., in an engine mount, air intake and exhaust system), and the receiver responses are sound pressure (P_t) or vibration, (e.g., in-vehicle noise at the driver's ear, and structural vibration) [12,23].

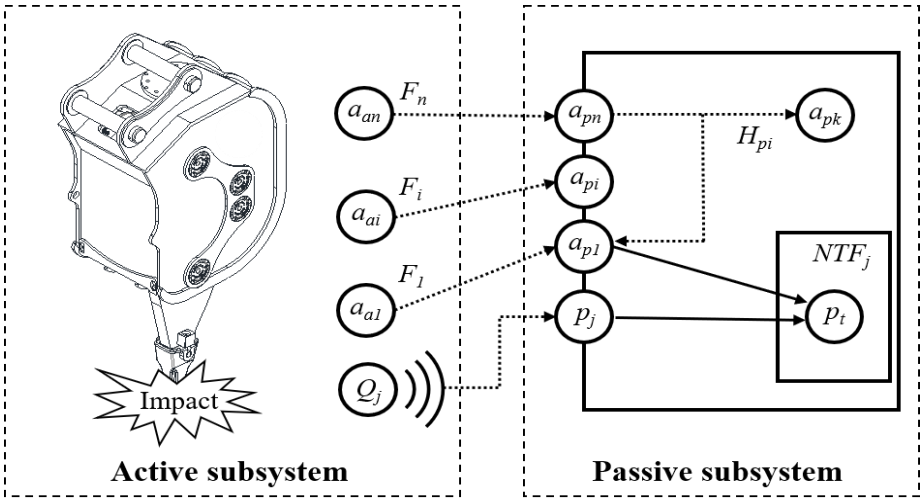

Figure 3. Schematic diagram of the TPA method showing an active subsystem generating structural and acoustic loads, and a passive subsystem responding to these loads (modified from Song et al. [12]).

The paths are represented by their corresponding frequency response functions (FRFs), which are often called noise transfer functions. Each of them describes the relationship between one input Degree of Freedom (DoF) and one response DoF. The model also includes a passive subsystem of FRFs, denoted by (H_{pi}) in Figure 3, generally referred to as local FRFs. These FRFs express the relationship among the responses at the input degrees of freedom (a_{pn}, p_j) and also at additional response locations called overdetermination points (a_{pk}). This model assumes a causal load–response relationship and that all the FRFs are characteristics of the global subsystem [12,24].

2.2. Frequency Domain Analysis of TPA

The TPA can be calculated by using the frequency domain or the time domain, depending on the calculation method for analyzing the measured signal. The TPA method for load estimation and quantification varies with the type of experiment and analysis method (e.g., methods for matrix inversion, dynamic stiffness, and intensity). The FRF data obtained from excitation tests and modal impact experiments are commonly used. Equation (1) can be summarized into Equation (2) when you exclude the effect of acoustic. The simplified equation is a matrix inversion method that can predict the transmitted load using the frequency response of the structure.

$$P_t(\omega) = \sum_{i=1}^{n} VTF_i(\omega) \cdot F_i(\omega) \tag{2}$$

This study employed the FRF obtained through modal experiments, involving a matrix inversion method that uses the vibrational characteristics during operation of the transfer function and the vibro-ripper. The load was analyzed using matrix inversion approaches by substituting the mass term (i.e., Newton's second law of motion), with the transfer function. This approach has a range of uses in engineering [23]. The matrix inversion approach can be expressed using vibration characteristics (i.e., the acceleration value) acquired by operational vibration experiments and the inverse matrix of the transfer function, as given in Equations (2) and (3).

$$\begin{bmatrix} F_1 \\ \vdots \\ F_N \end{bmatrix} = \begin{bmatrix} \mathrm{H}_1 & \cdots & \mathrm{H}_{1\mathrm{N}} \\ \vdots & \ddots & \vdots \\ \mathrm{H}_{\mathrm{M1}} & \cdots & \mathrm{H}_{\mathrm{MN}} \end{bmatrix} \cdot \begin{bmatrix} \ddot{x}_1 \\ \vdots \\ \ddot{x}_M \end{bmatrix} \tag{3}$$

$$\begin{bmatrix} F_1 \\ \vdots \\ F_N \end{bmatrix} = \begin{bmatrix} \mathrm{H}_1 & \cdots & \mathrm{H}_{1\mathrm{N}} \\ \vdots & \ddots & \vdots \\ \mathrm{H}_{\mathrm{M1}} & \cdots & \mathrm{H}_{\mathrm{MN}} \end{bmatrix}^{-1} \cdot \begin{bmatrix} \ddot{x}_1 \\ \vdots \\ \ddot{x}_M \end{bmatrix} \tag{4}$$

Here, $[F_N]$ is the excitation force, $[\mathrm{H_{MN}}]$ is an $m \times n$ transfer function matrix obtained through the modal impact experiments that describes the characteristics of the structure, and $\left[\ddot{x}\right]$ is the vibration characteristics of the structure. For the details of the TPA technique, refer to Song et al. [12].

2.3. Time Domain Analysis of TPA

The time domain analysis of the TPA method uses time signal data. The analysis in the time domain, the section where multiplication is applied in the frequency domain instead is applied by using the convolution integral within the time domain. Convolution is used to obtain the output signal, $y(t)$, about the input signal, $x(t)$, by using the response, $h(t)$, within the linear time-invariant system.

$$\mathrm{y}(t) = x(t) \cdot h(t) = \int x(t) \cdot h(t - \tau)\, d\tau \tag{5}$$

Here, $h(t - \tau)$ is the impulse function in the continuous system. It is defined as the convolution sum in a discrete system as expressed as follows;

$$\mathrm{y}[n] = x[n] \cdot h[n] = \sum_{k=-\infty}^{\infty} x[k] \cdot h[n - k] \tag{6}$$

where, $y[n]$ is the discrete output signal, $x[n]$ is the discrete input signal, and $h[n]$ is the impulse response of the discrete system. The function $h[n - k]$ represents the discrete unit-impulse function, which also includes the time invariance. Additionally, τ and k are arbitrary variables [12].

2.4. Vibration Experiment Setup

We analyzed the natural characteristics of a vibro-ripper and quantitatively estimated the impact loads transmitted to each of its components in a vibrational experiment. The vibrations during rock crushing were measured using an accelerometer (Figure 4a) attached at a position representing the shape of the vibro-ripper.

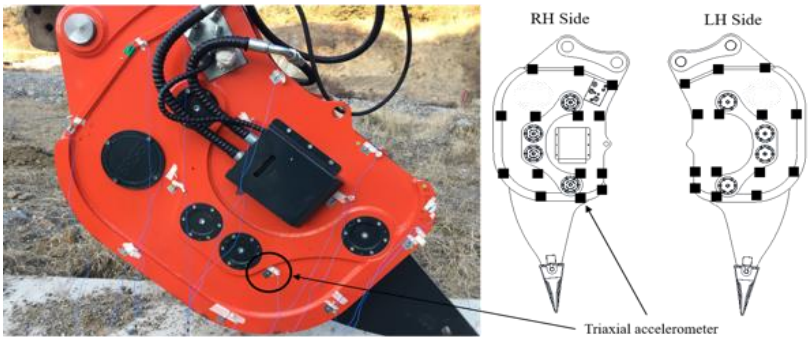

(**a**)

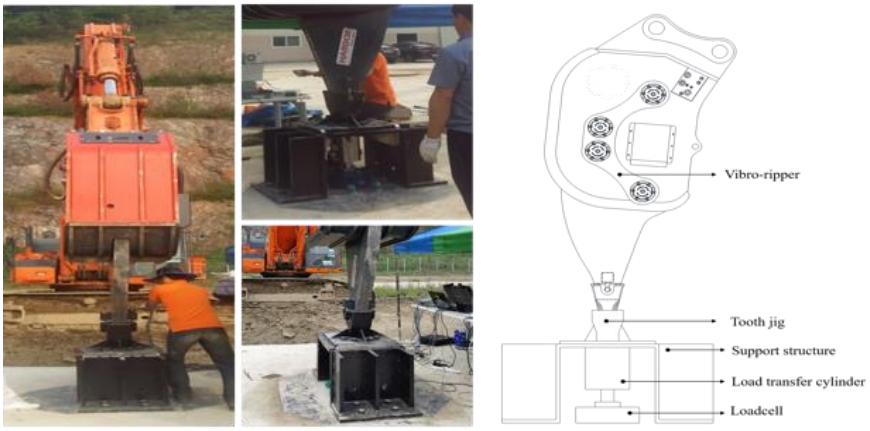

(**b**)

Figure 4. Vibration experiment setup. (**a**) positions of the installed tri-axial accelerometers; (**b**) Testing jig for impact load measurement.

The sensor employed in this study was a triaxial accelerometer that is suitable for high-impact experimental environments, using 84 channels. Data acquisition and analysis were managed by a supervisory control and data acquisition system (SCADAS) for overall experimental control, and a mobile data acquisition system with Test.lab software version 18.2 (Siemens, Munich, Germany). Experimental and operational conditions of the excavator and vibro-ripper are provided in Table 1. Table 2 lists the vibro-ripper's specifications.

Table 1. Parameters for vibrational experiments and operating conditions of the vibro-ripper.

Items	Parameters	Values
Tracking	Measurement method	Time trace
	Duration	30 s
	Increment	0.5 s
Acquisition	Bandwidth	6400 Hz
	Resolution	4 Hz
Vibro-ripper	Flow rate	290 lpm
	Working pressure	200 kg/cm^2
	Rotational speed	900 rpm

Table 2. Specifications of the vibro-ripper.

Model	Specifications	Values
BR-55	Applicable excavator	42–52 ton
	Frequency	Max. 28 Hz
	Working pressure	250 kg/cm^2
	Oil flow rate	290–310 lpm
	Weight	5200 kg

A vibro-ripper functions by converting the energy of a hydraulic motor into the kinetic energy of the shank and tooth, thereby breaking the rock. The vibro-ripper used in this study strikes the tooth jig connected to the steel structure (Figure 4b), to create uniform impact loads. The actual rock has mechanical properties that change due to anisotropy and irregularity [25]. Therefore, the uniformity and reproducibility of the test were ensured by minimizing the variation in the strength of the construction objects.

To ensure experimental reproducibility and repeatability, we constructed in situ testing equipment that enabled us to minimize variations in impact load related to the compressive strength of the rock (Figure 4b). The experiment design also eliminated effects related to inhomogeneity and anisotropy of the rock.

Striking of the tooth jig was expected to generate higher striking forces than during striking of the rock surface, as impact energy used to break the rock is transmitted to the housing of the vibro-ripper as a reaction force (in addition to energy dissipated as noise vibration, and hydraulic heat). To assess the effects of impact loads related to rock strength, it is necessary to conduct additional experiments using actual rock specimens. Data from sensor No. 12 during operation are shown in Figure 5 for vibration signals in the Z-direction (the main working direction) with respect to time.

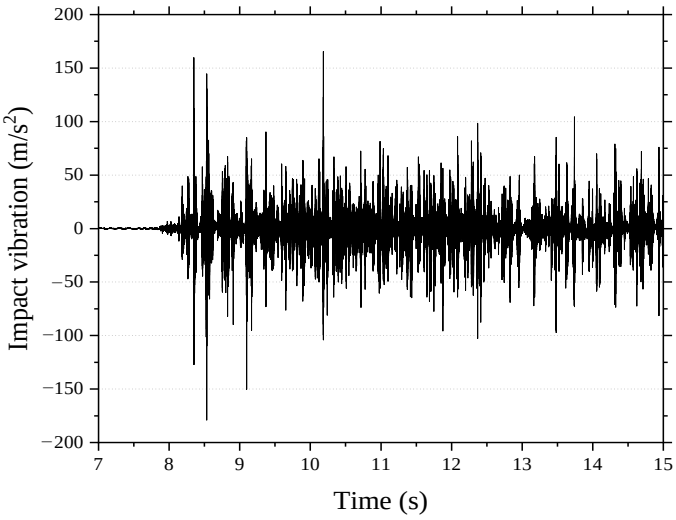

Figure 5. Measured impact vibration signal from the operating vibro-ripper.

2.5. Striking Force Measurement

To assess the impact loads transmitted to the housing of the vibro-ripper through the link modules, we need experimental data on the shank and tooth striking force, which can be used to validate the TPA calculation results. Therefore, a load measurement method using a load cell was adopted in deriving the impact load generated from the shank and tooth.

A test device including a load cell was constructed as shown in Figure 4b to measure the striking force of the vibro-ripper. A schematic diagram of the in situ test device is shown in Figure 4b. Test conditions for measurements of the impact load of the vibro-ripper and the main specifications of the load cell sensor are summarized in Table 3. Results

of measurements of the impact load of the vibrating ripper are shown in Figure 6. The maximum, minimum, and average values were 260, 180, and 220 kN, respectively.

Table 3. Specifications of the load cell sensor.

Model	Specification	Value
ULM-T100	Capacity	100 tonf (980.7 kN)
	Compensated temperature range	−10~60 °C
	Nonlinearity	0.05% R.O.
	Hysteresis	0.05% R.O.
	Repeatability	0.03% R.O.
	Diameter	310 mm
	Height	130 mm
	Weight	60 kg

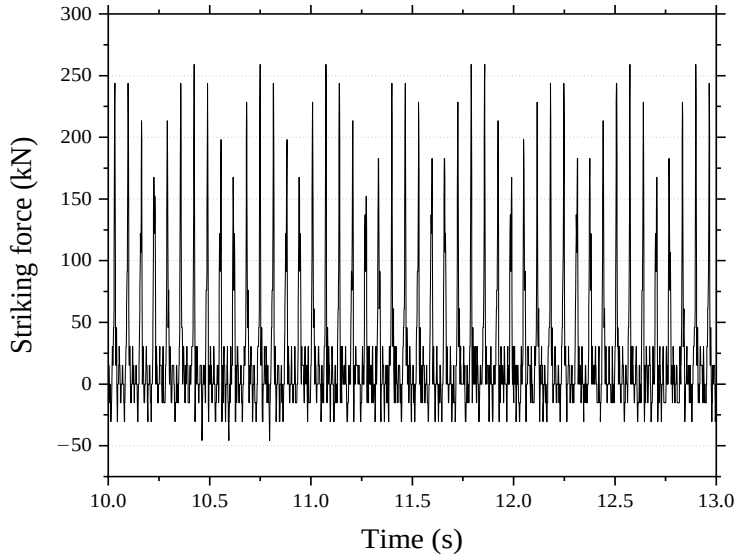

Figure 6. Results of striking force measurement via the load cell.

2.6. Selection of Load Transfer Path

The structure of the vibro-ripper receives the striking force through the link modules, and the eccentric gear mounted on the rotating shaft. The shank and tooth that receive the impact force hit the rock in the crushing operation. Due to the structure and operation characteristics of the vibro-ripper, the gearbox that generates the striking force (i.e., the medium that transmits the load between the vibration source and the housing) is where the link modules are mounted in four places on the left (LH side) and right (RH side). During ripper operation, the reaction force generated by the strength of the rock is transmitted to the housing through the shank and link module, so the position of the link module in the assembly was considered here as the main path of load transmission (Figure 7).

Transfer path analysis employs calculations founded on the characteristics of operational vibrations, and the transfer function matrix $[\mathbf{H}_{MN}]$ gained by a modal experiment of the structural path. The path is the medium that transmits the load between the gearbox (i.e., the excitation source) and the ripper's housing. Calculation of the load transmitted by this medium requires the characteristics of the principal contributing medium. Consequently, we considered all paths contributing to load transmission in the vibro-ripper (Figure 7).

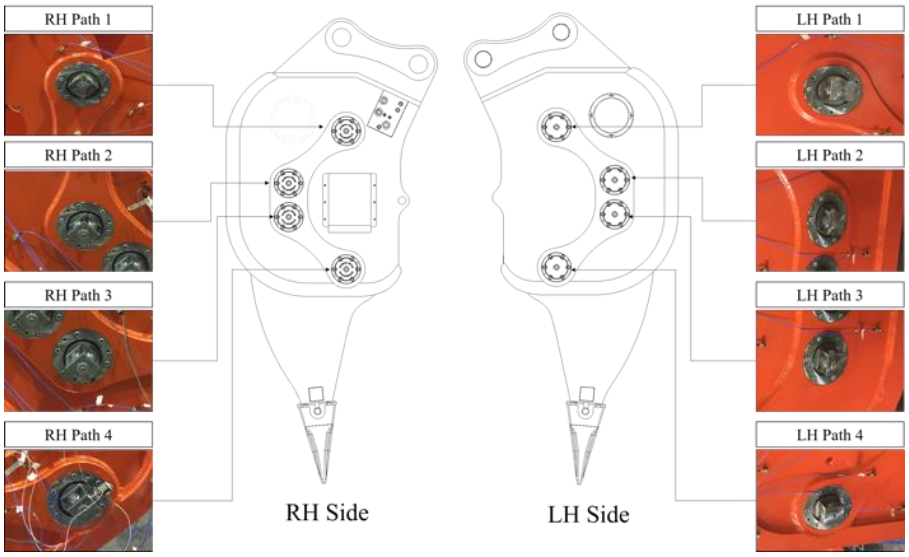

Figure 7. Positions of key paths in the vibro-ripper and triaxial excitation jig for frequency response function acquisition.

A modal-experiment jig, identical in shape to the link part, was developed to investigate the transfer path in triaxial excitations, for each position (Figure 7). The main load was applied horizontally during vibro-ripper operation. The impact load was transmitted to each part through triaxial vibration (roll, pitch, and yaw), induced by rock crushing. To analyze impact loads transmitted on the X, Y, and Z axes [12], modal impact experiments were undertaken to provide path transfer functions reflecting the main contribution to rock crushing. Attachment positions of the acceleration sensors in the experiment are shown in Figure 8, with a total of 84 sensor channels.

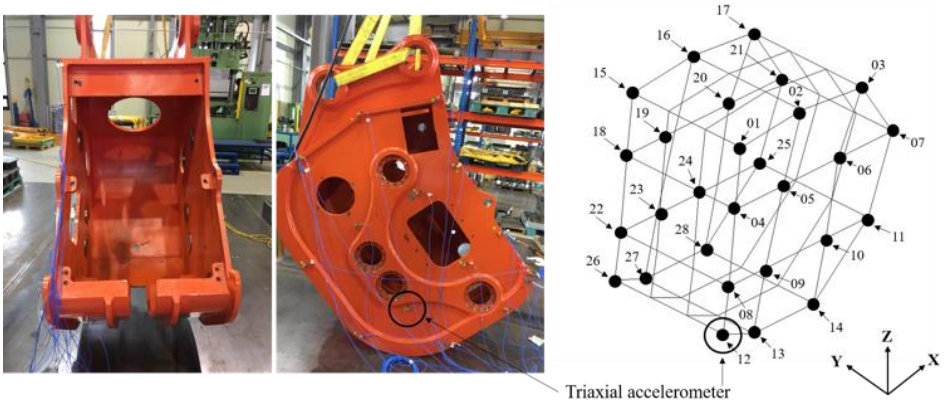

Figure 8. Installation sites of triaxial accelerometers in the modal experiment.

2.7. Acquisition of Transfer Function in the Modal Experiment

Analysis of the transfer path of vibration-based load requires a transfer function, which is a unique characteristic of the target system. The frequency response function (FRF) matrix obtained through the modal experiment provided the mass, strength, and damping matrices of the structure, enabling the derivation of characteristics of the dynamic system [12].

The modal experiment was undertaken to set the position of excitation in FRF matrices along the Y direction at the bottom end of the housing of the vibro-ripper. The experiments confirmed the unique characteristics of the housing in setting the excitation position (Figure 9a). The transfer function obtained in the modal impact experiment was applied to the assembly position of the link module, which makes a large contribution to load transfer

in the vibro-ripper (Figure 9a); the shank and teeth for rock striking are operated via the gearbox and link module.

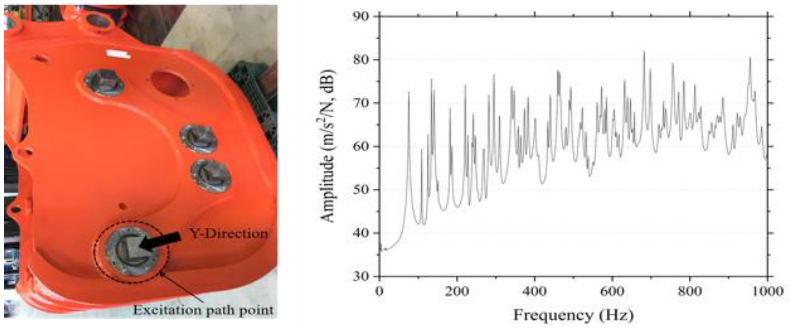

(**a**)

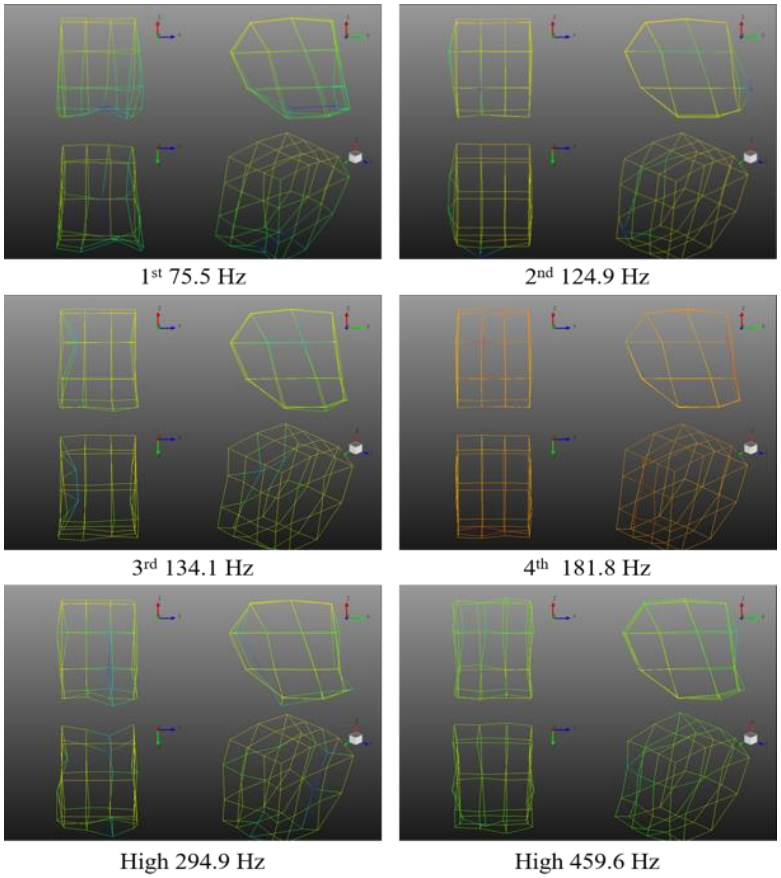

(**b**)

Figure 9. Results of the modal experiment. (**a**) frequency response function; (**b**) mode shapes of the ripper housing.

Examination of the major modal characteristics of the housing, including the position of the link module (Figure 9b), indicated that the bending mode occurred often in all frequency bands due to the overall shape of the housing. Mode shapes and their respective frequencies are provided in Table 4. The transfer function obtained by excitation of all paths (left and right) was applied in the TPA.

Table 4. Results of the modal experiment.

Mode No.	Mode Shapes	Natural Frequency (Hz)
1	Bending and torsion	75.5
2	Bending	124.9
3	Bending	134.1
4	Bending	181.8
High	Bending	294.9
High	Torsion	459.6

3. Results and Discussion

Vibration-based TPA was used to derive the loads in each direction and in link modules to quantify the impact load and its contributions to load transfer during vibro-ripper rock crushing.

Variations in impact load generated in the housing through the link modules over a 0.6 s timespan are shown in Figure 10. Time-domain TPA showed the loads to be transmitted to the ripper housing, with quantitative values provided in Table 5. Directional contributions to the impact transmission were analyzed in estimating loads generated and transmitted in the X, Y, and Z directions, yielding values of 67.1, 59.1, and 67.5 kN, respectively.

Table 5. Quantitative analysis results for impact load transmitted to the housing through each path.

Path No.	Axis	Load (kN)		Maximum Load (kN)
		+Dir.	−Dir	
LH Path 1	X	7.6	7.8	7.8
	Y	7.4	7.0	7.4
	Z	1.5	1.3	1.5
LH Path 2	X	8.1	8.1	8.1
	Y	6.3	4.8	6.3
	Z	11.3	10.7	11.3
LH Path 3	X	9.7	11.3	11.3
	Y	9.4	9.2	9.4
	Z	8.1	9.5	9.5
LH Path 4	X	5.2	5.4	5.4
	Y	5.5	5.6	5.6
	Z	10.6	8.5	10.6
RH Path 1	X	8.0	8.2	8.2
	Y	7.4	7.9	7.9
	Z	1.6	1.3	1.6
RH Path 2	X	8.6	8.5	8.6
	Y	5.0	6.6	6.6
	Z	11.9	11.2	11.9
RH Path 3	X	10.2	11.9	11.9
	Y	9.6	10.0	10.0
	Z	8.6	10.0	10.0
RH Path 4	X	5.5	5.7	5.7
	Y	5.9	5.8	5.9
	Z	11.1	9.0	11.1

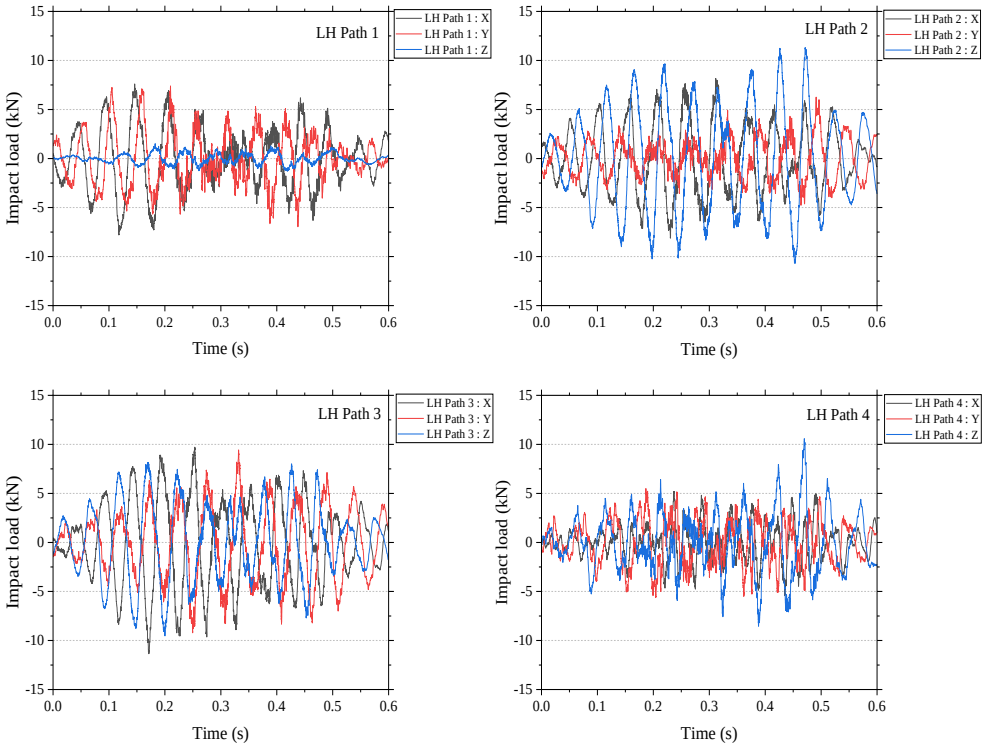

(**a**)

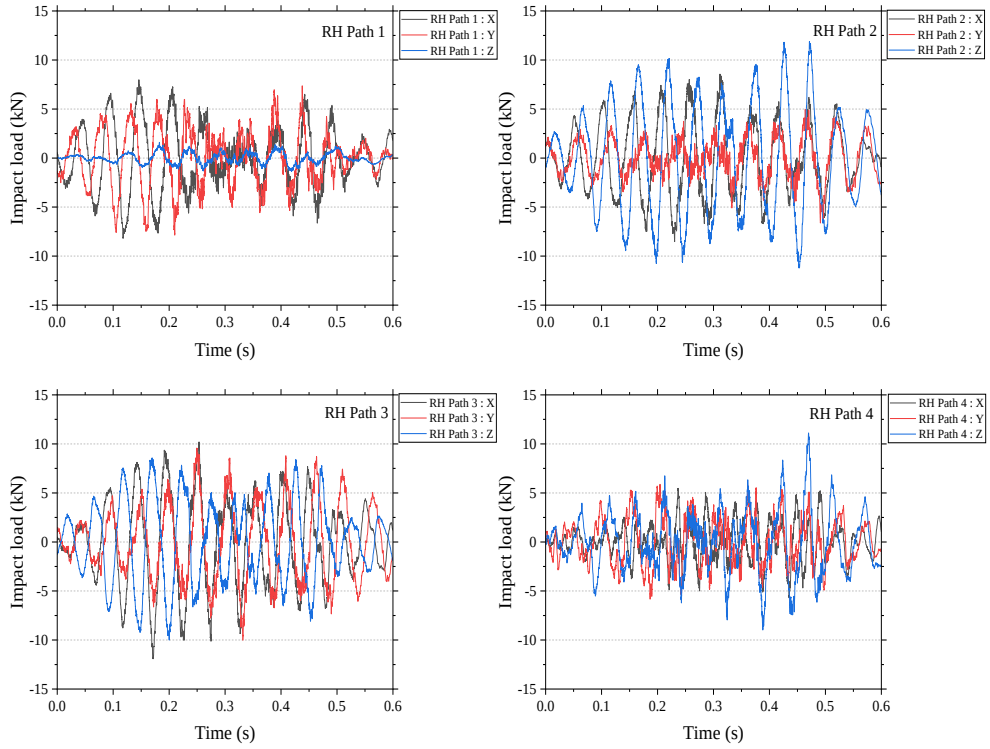

(**b**)

Figure 10. Calculated impact load profile for each path of the vibro-ripper. (**a**) LH path; (**b**) RH path.

Analysis results are shown in Figure 11 for the frequency domain, representing the contribution of each major path to the final load transmitted to the housing during ripper operation. The results indicate that the main contributions were made in the X and Z directions with respect to load transmission, with a relatively small contribution in the

Y direction owing to the motion of the shank assembly being mainly in these directions. Furthermore, the maximum load occurred in the frequency domain of ~50 Hz, whereas the load transmitted to the housing was relatively insignificant at frequencies above 100 Hz.

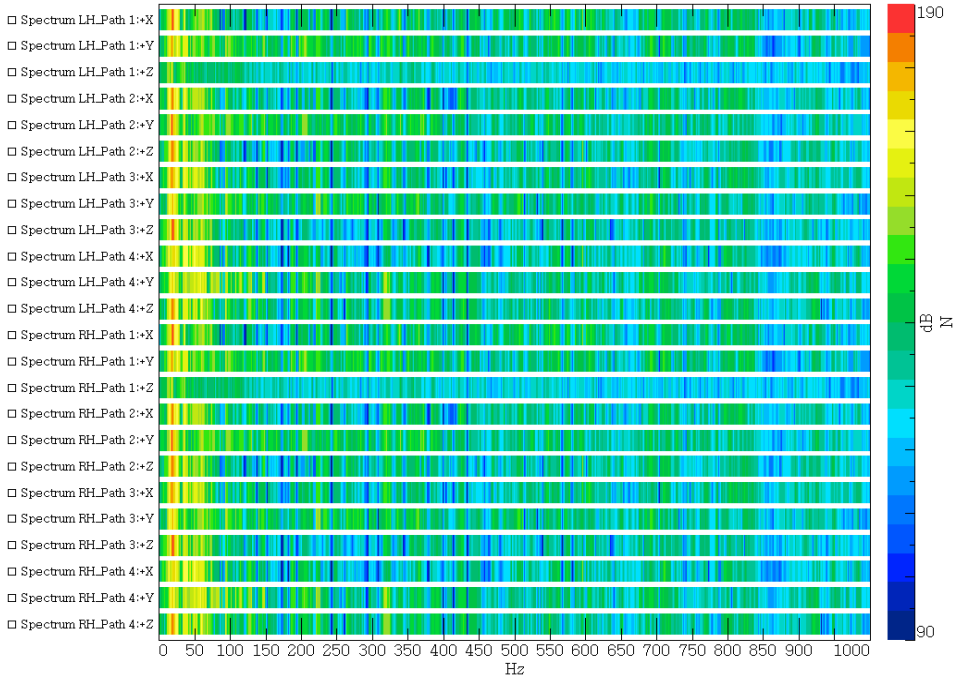

Figure 11. Relative contributions of impact loads conveyed to the housing through each path.

The TPA method yielded an impact load of 193.7 kN, compared with the striking force of 220 kN measured using the load cell (a difference of 12.3%). Thus, the reaction force produced during striking by the shank was damped mainly by the gearbox and isolation rubber and was ultimately transmitted via the link modules to the housing. The results confirm the applicability of the TPA method to a structure with impact loads and vibration. This method accounts for energy loss as a result of vibration, noise, hydraulic heat, and reaction force during shank striking work. An evaluation of the reliability of this method requires additional study using computational and numerical engineering approaches to assess load transfer through the link modules, as well as further tests of the material properties of the link modules.

Additional analyses employing load estimation and evaluation techniques might lead to the development of a new method for evaluating the life-cycle durability of key parts of rock-crushing devices, with the operational state of various parts being closely related to the durability and performance of mechanical equipment. In addition, the impact loads of this study relevant to each component and direction can be used as input parameters for numerical analyses of vibro-rippers.

This study did not consider the Load Transfer Characteristics of structure materials and the dynamic response of components during the working process of the vibro-ripper. Overcoming this limitation would require an assessment of the reliability of the load estimates through vibration-based TPA by introducing the computer aided engineering (CAE) method, which considers the physical properties and dynamic response of the ripper's components.

4. Conclusions

A vibration-based transfer path analysis method was developed for estimating impact loads generated during vibro-ripper operation. Impact loads in each direction and on each part of a vibro-ripper were estimated quantitatively during its operation, and the contribution of loads generated by and transmitted to link modules analyzed.

The contribution of impact loads in each component was evaluated by a load contribution map (Figure 11). Using the load contribution map, we analyzed the frequency bands that are commonly used for load transfer. The frequency bands above 50 Hz showed a minor effect of impact loads transmitted to the housing. The applicability of the TPA method to a mechanical system with impact vibrations and loads was verified by comparison of the striking force of the shank, measured from a load cell, with transmitted loads calculated using the TPA method. Results of this study may be important input values for numerical analysis in equipment design and can be used as key data for structural safety evaluation and optimization.

Further verification experiments are required to verify the validity of the proposed load estimation method, and further studies employing the vibration-based load measurement and evaluation methods used here for rotating bodies could lead to new concepts for estimation of operating loads in construction machines whose loads are difficult to measure.

Author Contributions: Conceptualization, J.C. and C.S.; methodology, C.S. and D.K.; software, C.S. and D.K.; validation, H.-J.P., J.-Y.O. and J.-W.C.; formal analysis, C.S. and D.K.; investigation, C.S., D.K. and H.-J.P.; resources, J.-Y.O. and J.-W.C.; data curation, H.-J.P.; writing—original draft preparation, C.S. and D.K.; writing—review and editing, J.C. and C.S.; visualization, D.K and H.-J.P.; supervision, C.S.; project administration, J.-Y.O. and J.C.; funding acquisition, J.-Y.O. and J.C. All authors have read and agreed to the published version of the manuscript.

Funding: This work was conducted with the support of the "National R&D Project for Smart Construction Technology (No.1615013104)" funded by the Korea Agency for Infrastructure Technology Advancement under the Ministry of Land, Infrastructure and Transport, and managed by the Korea Expressway Corporation. Additionally, this work was supported by a National Research Foundation of Korea (NRF) grant funded by the Korean government (MEST) (NRF-2021R1A2C2007979).

Institutional Review Board Statement: Not applicable.

Informed Consent Statement: Not applicable.

Data Availability Statement: Not applicable.

Acknowledgments: We would like to express our special thanks to Hankwon Lee for advice on experimental design and data analysis.

Conflicts of Interest: The authors declare no conflict of interest.

References

1. Jonck, J.; Slabbert, G.A. Analysis of a failed spur gear from a vibro-hammer. *Eng. Fail. Anal.* **2013**, *34*, 511–518. [CrossRef]
2. Chen, F.Q.; Wang, J.W.; Li, D.Y.; Qiao, W.G. Application and advance of vibratory driving techniques using high-frequency hydraulic vibratory hammer. *Chin. J. Geotech. Eng.* **2011**, *33*, 224–231. (In Chinese)
3. Xu, G.N.; He, M.; Wu, J.F. Transient vibration analysis of impact ripper. *Appl. Mech. Mater.* **2014**, *551*, 150–157. [CrossRef]
4. Oh, K.K.; Kim, J.; Park, J.Y.; Yang, G.; Park, J.; Kim, S.H. Evaluation of fatigue life of welded joint of gear box-shank in vibro ripper using PSN curve. *Trans. Korean Soc. Mech. Eng. A* **2015**, *39*, 1207–1212. (In Korean) [CrossRef]
5. Lee, S.; Yoon, K.; Kim, E. A Study on Mechanical Vibrational Properties of Vibro-hammer. *J. Korean Soc. Hazard Mitig.* **2013**, *13*, 107–112. (In Korean) [CrossRef]
6. Ficarella, A.; Giuffrida, A.; Laforgia, D. Numerical investigations on the working cycle of a hydraulic breaker: Off-design performance and influence of design parameters. *Int. J. Fluid Power* **2006**, *7*, 41–50. [CrossRef]
7. Ficarella, A.; Giuffrida, A.; Laforgia, D. Investigation on the impact energy of a hydraulic breaker. In *SAE Technical Paper*; SAE International: Warrendale, PA, USA, 2007.
8. Ficarella, A.; Giuffrida, A.; Laforgia, D. The effects of distributor and striking mass on the performance of a hydraulic impact machine. In *SAE Technical Paper*; SAE International: Warrendale, PA, USA, 2008.
9. Lee, S.H.; Han, C.S.; Song, C.S. A study on the performance improvement of a high efficiency hydraulic breaker. *J. Korean Soc. Tribol. Lubr. Eng.* **2003**, *19*, 59–64.
10. Kim, B.S.; Kim, M.G.; Byun, D.W.; Lee, S.M.; Lee, S.H. A study on the structure improvement of bracket housing for structural noise and vibration reduction in hydraulic. *J. Korean Soc. Precis. Eng.* **2006**, *23*, 108–115. (In Korean)
11. Park, G.B.; Park, C.H.; Park, Y.S.; Choi, D.H. Optimal design for minimizing weight of housing of hydraulic breaker. *Trans. Korean Soc. Mech. Eng. A* **2011**, *35*, 207–212. (In Korean) [CrossRef]

12. Song, C.; Kim, D.J.; Chung, J.; Lee, K.W.; Kweon, S.S.; Kang, Y.K. Estimation of impact loads in a hydraulic breaker by transfer path analysis. *Shock Vib.* **2017**, *2017*, 8564381. [CrossRef]
13. Baker, W.E.; Dove, R.C. Measurement of internal strain in a bar subjected to longitudinal impact. *Exp. Mech.* **1962**, *2*, 307–311. [CrossRef]
14. Suzuki, S. Measured dynamic-load factors of cantilever beams, frame structures and rings subjected to impact loads. *Exp. Mech.* **1971**, *11*, 76–81. [CrossRef]
15. Knapp, J.; Altmann, E.; Niemann, J.; Wemer, K.D. Measurement of shock events by means of strain gauges and accelerometers. *Measurement* **1998**, *24*, 87–96. [CrossRef]
16. Shepherd, C.J.; Thomas, G.J.A.; Wilgeroth, J.M.; Hazell, P.J.; Allsop, D.F. On the response of ballistic soap to one-dimensional shock loading. *Int. J. Impact Eng.* **2011**, *38*, 981–988. [CrossRef]
17. Xue, X.; Ren, T.; Zhang, W. Analysis of fatigue damage character of soil under impact load. *J. Vib. Control* **2013**, *19*, 1728–1737. [CrossRef]
18. Hashiba, K.; Fukui, K.; Liang, Y.Z.; Koizumi, M.; Matsuda, T. Force-penetration curves of a button bit generated during impact penetration into rock. *Int. J. Impact Eng.* **2015**, *85*, 45–56. [CrossRef]
19. Zhang, J.; Guo, S.L.; Wu, Z.S.; Zhang, Q.Q. Structural identification and damage detection through long-gauge strain measurements. *Eng. Struct.* **2015**, *99*, 173–183. [CrossRef]
20. Asbjörnsson, G.; Bengtsson, M.; Hulthén, E.; Evertsson, M. Modelling of discrete downtime in continuous crushing operation. *Miner. Eng.* **2016**, *98*, 22–29. [CrossRef]
21. Kim, S.J.; Lee, S.K. Prediction of interior noise by excitation force of the powertrain based on hybrid transfer path analysis. *Int. J. Automot. Technol.* **2008**, *9*, 577–583. [CrossRef]
22. SIEMENS. Technical Info Issued: What is Transfer Path Analysis. 2014. Available online: http://www.plm.automation.siemens.com/en_us/products/lms/testing/transfer-path-analysis.shtml#lightview-close (accessed on 10 May 2017).
23. Qian, K.; Hou, Z.; Liang, J.; Liu, R.; Sun, D. Interior sound quality prediction of pure electric vehicles based on transfer path synthesis. *Appl. Sci.* **2021**, *11*, 4385. [CrossRef]
24. Gajdatsy, P.; Janssens, K.; Desmet, W.; Auweraer, H.V. Application of the transmissibility concept in transfer path analysis. *Mech. Syst. Signal Process.* **2010**, *24*, 1963–1976. [CrossRef]
25. Kahraman, S.; Bilgin, N.; Feridunoglu, C. Dominant rock properties affecting the penetration rate of percussive drills. *Int. J. Rock Mech. Min. Sci.* **2003**, *40*, 711–723. [CrossRef]